

The electronic structure and optical properties of  $m-ZrO_2$ ,  $t-ZrO_2$ ,  $c-ZrO_2$  and fluorite-related  $Zr_2ON_2$  compounds are studied using the functional density theory with the generalized gradient approximation (GGA) parameterized with the revised Perdew-Burke-Ernzerh for solids as an exchange correlation function. We found that hybridization among the Zr-d, O-p and N-p states results in the formation of a covalent bond between Zr-N and Zr-O. The calculated optical properties confirm that the  $Zr_2ON_2$  is an active photocatalyst under visible light irradiation. A high refractive index of 2.0 at 650 nm is obtained which shows better agreement with the experimental value (2.2 at 650 nm) than previous results.

## 1. INTRODUCTION

In recent years, there has been a growing interest in replacing metallic parts in heat engines by structural ceramics such as zirconium dioxide ( $ZrO_2$ ) [1]. However, the high-temperature form of  $ZrO_2$  with the fluorite structure and high oxide ion mobility is unstable at room temperature. One approach to stabilise the fluorite structure of  $ZrO_2$  is aliovalent substitution of  $Zr^{4+}$  by  $Y^{3+}$  or  $Ca^{2+}$  [2, 3]. As well as stabilising the fluorite structure, this introduces anion vacancies enhancing the oxide ion conductivity. A second approach is to make an anion substitution of  $O^{2-}$  by  $N^{3-}$  to make a series of zirconium oxynitrides which will have anion vacancies [4]. First principle studies are optimistic approaches, which provide better experimental parameters leading to rapid material improvements economically. In the present work we propose a comprehensive study about electronic and elastic properties of zirconium dioxide ( $ZrO_2$ ) in the monoclinic, tetragonal and cubic phases and the fluorite-related zirconium oxynitride ( $Zr_2ON_2$ ) by ab initio study.

## 2. COMPUTATIONAL DETAILS

CASTEP (Cambridge Serial Total Energy Package) software [5] was utilized in our calculations, based on density functional theory (DFT). CASTEP uses a plane wave basis set for the expansion of the single particle Kohn-Sham as implemented and ultra-soft pseudo potentials to describe ionic cores. The minimum total energy of the structure is achieved by relaxing automatically the internal coordinates using the Broyden-Fletcher-Goldfarb-Shanno (BFGS) algorithm. The atomic configurations of Zr, O and N generated from the ultrasoft pseudopotential are  $4s^2 4p^6 4d^2 5s^2, 2s^2 2p^4$  and  $2s^2 2p^3$ , respectively. The exchange correlation energy is described by Generalized Gradient Approximation (GGA) of the revised Perdew-Burke-Ernzerh for solids (PBESOL) [6]. Brillouin zone sampling is performed using  $3 \times 3 \times 3$ ,  $4 \times 4 \times 3$ ,  $3 \times 3 \times 3$  and  $1 \times 1 \times 1$  Monkhorst-Pack k-points meshes for cubic, tetragonal, monoclinic  $ZrO_2$  and fluorite-related  $Zr_2ON_2$ , respectively. The plane wave cut off energy in our calculations is 380 eV, which assures a total energy convergence of  $5.0 \times 10^{-7}$  eV/atom.

## 3. RESULTS AND DISCUSSION

The minimization of the total energy leads to the equilibrium lattice constant of  $ZrO_2$  and  $Zr_2ON_2$ . The calculated equilibrium lattice parameters ( $a_0, b_0, c_0; V_0$ ) and band structure for these structures are presented in Table 1 and compared with the experimental values. The results obtained after structural and atomic relaxation as shown in Table 1 are found to be in agreement with the crystal structure obtained from diffraction experiments [7-10].

Table 1: Lattice parameters of  $m-ZrO_2$ ,  $t-ZrO_2$ ,  $c-ZrO_2$  and  $Zr_2ON_2$  compared to experiment results

	$m-ZrO_2$		$t-ZrO_2$		$c-ZrO_2$		$Zr_2ON_2$	
	This study	Expt	This study	Expt	This study	Expt	This study	Expt
$a_0$	5.132	5.17 [7]	3.587	3.57 [8]	5.06	5.09 [9]	10.104	10.139 [10]
$c_0$	5.303	5.14	5.185	5.16	-	-	10.117	-
$b_0$	5.214	5.20	-	-	-	-	10.040	-
$V_0$	141.9	138.18	66.7	70.5	129.55	131.87	1026.40	1042.41

### 3.1. Electronic structure

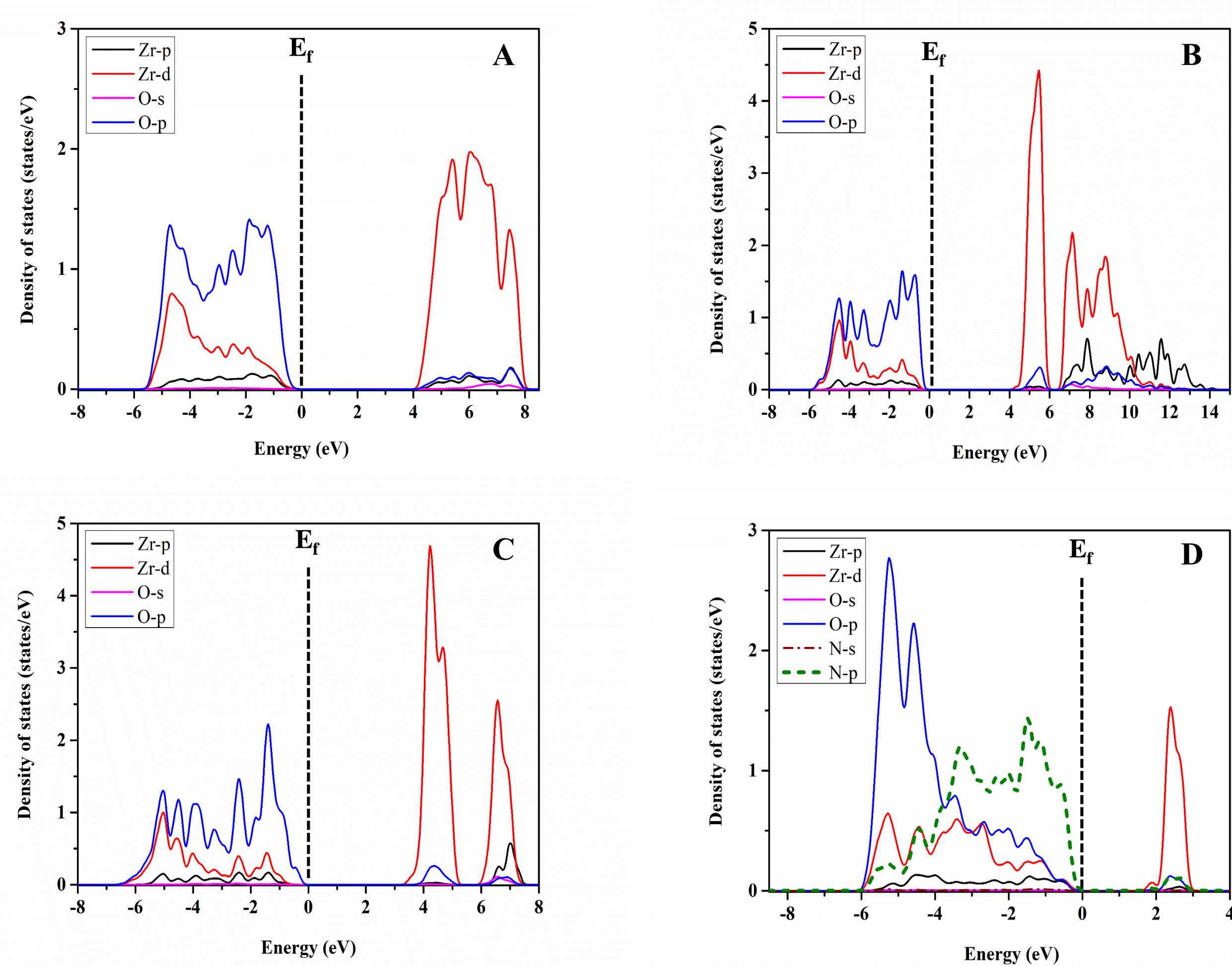


Figure 1. PDOS of: (A)  $m-ZrO_2$ , (B)  $t-ZrO_2$ , (C)  $c-ZrO_2$  and (D) fluorite-related  $Zr_2ON_2$  compounds

The partial density of states of  $m-ZrO_2$ ,  $t-ZrO_2$ ,  $c-ZrO_2$  and  $Zr_2ON_2$  are presented in figure 1. The dotted represents the Fermi level ( $E_f$ ), which is set to zero. Band gaps of 3.97, 4.01, 3.3 and 1.55 eV are obtained respectively for these phases. The underestimation of band gaps by DFT is common, which exists due to the limitation of predicting conduction band properties. As a result, the conduction band minimum of  $Zr_2ON_2$  is reduced compared to  $ZrO_2$ , which makes  $Zr_2ON_2$  active under visible light irradiation.

For  $ZrO_2$  phases, the valence bands and the lower conduction bands are all quite similar but become more flat in going from the cubic to the monoclinic phase. The valence bands are composed with a higher mixed O 2p, Zr 4d orbitals of about 4 -6 eV width. The conduction band is mainly derived from the Zr 4d orbitals. For the  $Zr_2ON_2$  fluorite structure, the valence band maximum mostly consists of O 2p and N 2p states which are strongly hybridized with Zr 4d orbitals, while the bottom of the conduction band is composed of a Zr 4d state overlap with O 2p and N 2p. Strong hybridization means potential covalent bonding and a less ionic character. A covalent bond between O or N and the Zr atom can be seen when the O 2p and N 2p states hybridized with Zr 4d between -5.5 eV and 0.0 eV.

### 3.2 Optical properties

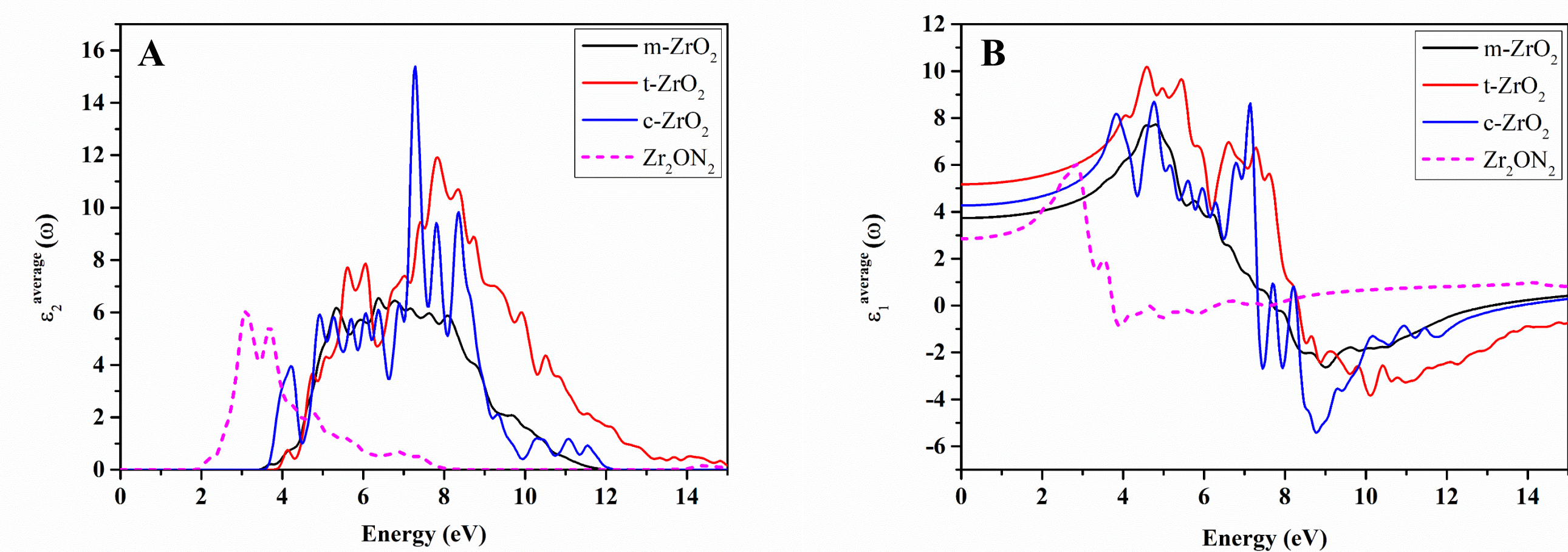


Figure 2. Calculated: (A)  $\epsilon_2^{average}$  and (B)  $\epsilon_1^{average}$  for  $m-ZrO_2$ ,  $t-ZrO_2$ ,  $c-ZrO_2$  and fluorite-related  $Zr_2ON_2$  compounds

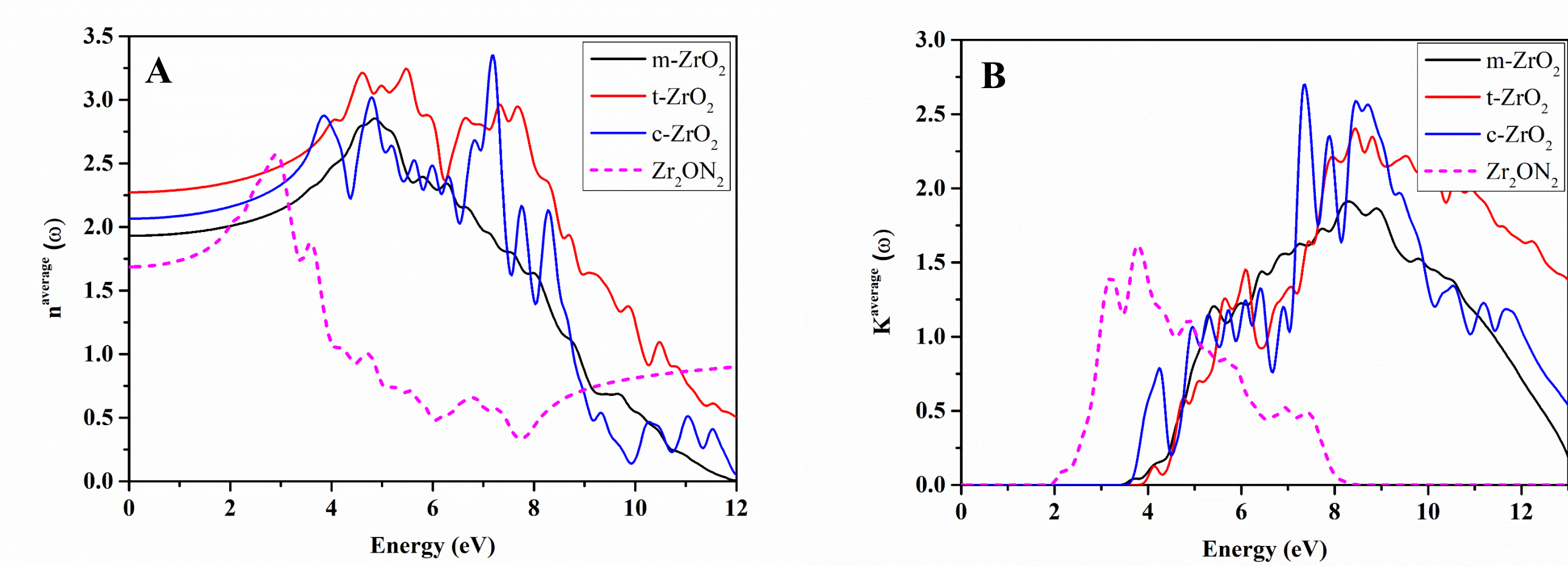


Figure 3. Refractive index and extinction coefficient. (A)  $n^{average}(\omega)$ , (B)  $K^{average}(\omega)$  for  $m-ZrO_2$ ,  $t-ZrO_2$ ,  $c-ZrO_2$  and fluorite-related  $Zr_2ON_2$  compounds

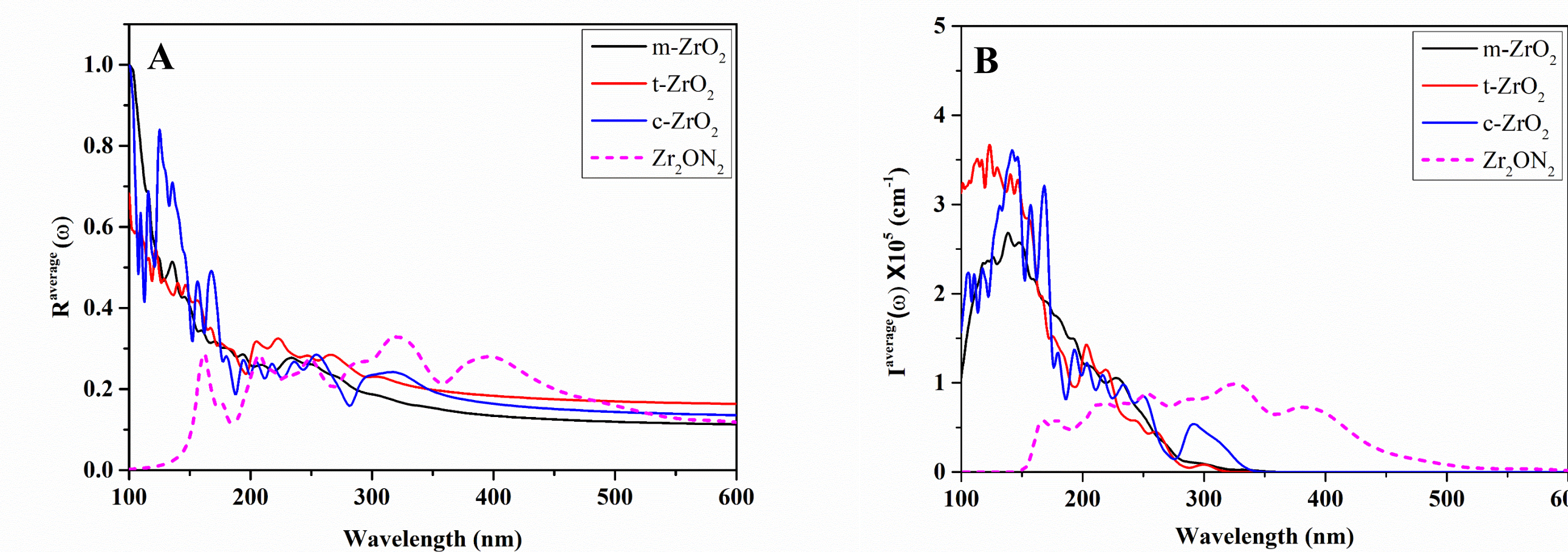


Figure 4. Reflectivity and absorption coefficient. (A)  $R^{average}(\omega)$ , (B)  $L^{average}(\omega)$  for  $m-ZrO_2$ ,  $t-ZrO_2$ ,  $c-ZrO_2$  and fluorite-related  $Zr_2ON_2$  compounds

The optical properties of  $ZrO_2$  and  $Zr_2ON_2$  are calculated by the dielectric function  $\epsilon(\omega) = \epsilon_1(\omega) + i\epsilon_2(\omega)$ . The Kramer-Kronig relation is used to obtain the real parts of the dielectric function from imaginary ones (Figure 2). Optical properties such as refractive index  $n(\omega)$ , extinction coefficient  $k(\omega)$ , reflectivity  $R(\omega)$  and absorption coefficient  $I(\omega)$  are calculated from the dielectric constant (Figure 3 and 4).

The average value of the refractive index of  $Zr_2ON_2$  is 1.7 at the static limit  $n^{average}(\omega)$  and 2.0 at 650 nm. Our calculations show better agreement with the experimental value, 2.2 at 650 nm [11], than another theoretical value. The refractive indices increased beyond the zero frequency limits and reached their maximum values. Beyond the maximum value they start to decrease and with a few oscillations they go beyond unity for all compounds. The maximum reflectivity value for  $ZrO_2$  compounds occurs at about 95, 75 and 90 nm for  $m-ZrO_2$ ,  $t-ZrO_2$ ,  $c-ZrO_2$ , respectively. On the other hand,  $Zr_2ON_2$  has a low reflectivity values compared to  $ZrO_2$  with maximum values occurs from 160 nm. The absorption coefficient,  $I(\omega)$ , measures the penetration of light through materials before it gets absorbed. We have calculated the absorption coefficient in terms of wavelength (nm) (see Figure 4 (B)). The  $I(\omega)$  rapidly increases above 100 nm for  $ZrO_2$  and 150 nm for  $Zr_2ON_2$ . Absorption also occurs in the visible region, which indicates that  $Zr_2ON_2$  is an active photocatalyst under visible light irradiation and the absorption band extends from 150 nm to 550 nm.

## 4. CONCLUSIONS

The electronic and optical properties of  $m-ZrO_2$ ,  $t-ZrO_2$ ,  $c-ZrO_2$  and fluorite-related  $Zr_2ON_2$  structures are explored using the first principles total energy plane wave pseudo potential method based on density functional theory.

The calculations show that  $Zr_2ON_2$  has a band gap value of 1.55 eV, and  $ZrO_2$  with the monoclinic and tetragonal structure have a band gap value of about 4 eV and 3.3 eV for the cubic structure. In the PDOS, the hybridized anion p and Zr-d orbitals are accountable for the covalent bond between Zr-N and Zr-O. As a consequence of this covalent bond, the valence band dispersion increases and pushes the top of the valence band towards the Fermi level, resulting in a  $Zr_2ON_2$  compound that is photocatalytically active under visible light irradiations. We found the refractive index to be about 2.0 at 650 nm for  $Zr_2ON_2$ , which is in good agreement with the experimental value (2.2 at 650 nm).

## 5. REFERENCES

- [1] D. J. Clough, Ceramic Engineering and Science Proceedings, 6 (1985)
- [2] X. J. Chen, K. A. Khor, S. H. Chan and L. Gyu, Materials Science and Engineering: A. 335 (2002) 246-252
- [3] F.A. Kroger Journal of the American ceramic society 49 (1966) 215-218
- [4] T. Bredow and M. Lerch, Journal of inorganic and general chemistry 630 (2004) 2262-2266
- [5] M. D. Segall, J. D. Lindan, M. J. Robert, C. J. Pickard, P. J. Hasnip, S. J. Clark and M. C. Payne. Journal of Physics: Condensed Matter, 14 (2002). 2717-2744.
- [6] J. P. Perdew, K. Burke and M. Ernzerhof, Physical Review Letters 78 (1997) 1396
- [7] M. N. Tahir, L. Gorgishvili, J. Li, T. Gorelik, U. Kolb, L. Nasdala and W. Tremel, Solid State Sciences 9 (2007) 1105-1109
- [8] P. Bouvier, E. Djurado, C. Ritter, A. J. Dianoux and G. Lucazeau, International Journal of Inorganic Materials 3 (2001) 647-654
- [9] G. Katz, Journal of the American ceramic society, 54 (1971) 531
- [10] S. J. Clarke, C. W. Michie, and M. J. Rosseinsky, Journal of Solid State Chemistry 146 (1999) 399-405
- [11] M. Laurikaitis, S. Burinskas, J. Dudonis and D. Milčius, Journal of Physics: Conference Series 100 (2008) 082051